Journal of Alloys and Compounds 749 (2018) 140–145

Contents lists available at ScienceDirect

Journal of Alloys and Compounds

journal homepage: http://www.elsevier.com/locate/jalcom

Retaining meta-stable fcc-Cr phase by restraining nucleation of equilibrium bcc-Cr phase in CuCrZrTi alloys during ageing

Hang Wang [a], Liukui Gong [b], Jinfa Liao [b], Huiming Chen [a], Weibin Xie [a], Bin Yang [a, *]

[a] National Engineering Research Centre for Copper Smelting and Manufacturing/Institute of Engineering Research, Jiangxi University of Science and Technology, Ganzhou, Jiangxi, 341000, PR China
[b] School of Materials Science and Engineering, Jiangxi University of Science and Technology, Ganzhou, Jiangxi, 341000, PR China

ARTICLE INFO

Article history:
Received 6 January 2018
Received in revised form
16 March 2018
Accepted 19 March 2018
Available online 22 March 2018

Keywords:
Cu-Cr based alloys
Precipitation
Nucleation
Atom probe tomography
Thermodynamic calculations

ABSTRACT

Cr-rich precipitates with a bcc crystal structure are an equilibrium phase in high-strength Cu–Cr alloys. Metastable fcc Cr-rich precipitates that are coherent with a fcc Cu matrix were retained in a Cu–Cr–Zr–Ti alloy during ageing. Atom-probe tomography analysis revealed that Cr atoms exist in the core of the Cr-rich precipitates, whereas Zr atoms segregate on the periphery. Fcc Cr-rich precipitates are prone to form because of the low nucleation barrier. A rapid diffusion of Ti atoms in the matrix stimulates the fcc Cr-rich nuclei growth. Resulting solute-lean zones hinder further nucleation of equilibrium bcc Cr-rich precipitates.

1. Introduction

Cu-Cr-Zr alloy has been recently widely used in nuclear industry and electrical industry [1–4]. Its high strength is mainly due to ageing precipitates of Cr [5]. It is reported that the role of Zr atoms in this type of alloy is either forming Cu_4Zr/Cu_5Zr precipitates or restraining growth of Cr precipitates [6]. As few Cu_4Zr/Cu_5Zr precipitate has been found and observed, it is believed that refinement of Cr precipitates by Zr atoms is responsible for strengthening Cu-Cr-Zr alloy [6,7]. This behaviour has been confirmed by atom probe tomography (APT) observation showing that Zr atoms locate on two sides of Cr precipitates leading to elliptic morphology with smaller size [8–10]. In addition, the addition of Zr to the Cu-Cr alloys improves the fatigue and creep properties of these alloys [11]. The improvement in fatigue and creep properties is ascribed to the Zr-atom-drag effect on grain boundary motion. Therefore, the Cu-Cr alloy containing Zr has better strength, fatigue and creep behaviour than conventional Cu-Cr system alloys [12].

Ti is also an important micro-alloying element which makes Cr precipitates in cigar shape (elliptic morphology) [6,13–15]. It is proposed that Ti atoms segregate on the surface of Cr precipitates which produces a sandwich structure [16], similar to the APT observation of Zr atoms [8–10]. However, in our previous work, Ti atoms are found to exist in Cr precipitates which increase the elastic strain energy resulting in cuboid morphology of the precipitates [17]. Since there has been no direct evidence showing where Ti atoms locate and how they influence the morphology of Cr precipitates. In another word, it is still unclear whether Ti atoms play the same role as Zr atoms. Therefore the morphology of Cr precipitates in Cu-Cr-Zr-Ti alloy has been characterised in the present work using atom probe tomography technology and high resolution transmission electron microscopy. The effect of the location of Ti atoms on the phase transformation of precipitates and mechanical property during ageing has also been investigated.

2. Experimental

Raw materials in the present work were pure Cu (99.95 wt%), pure Ti (99.99 wt%), Cu-1.6 wt%Cr alloy and Cu-70 wt%Zr alloy. Melting was conducted in air using medium frequency induction furnace (DS-7-003, Wuxi Doushan Furnace). Melting temperature was controlled at 1100 ± 10 °C. Molten was covered by charcoal to reduce oxidation before casting into graphite mould. The compositions of two as-cast ingots were measured using inductively coupled plasma emission spectroscopy (ICP, 8800, Agilent): Alloy 1

---

* Corresponding author.
E-mail address: yangbin65@126.com (B. Yang).

https://doi.org/10.1016/j.jallcom.2018.03.238

Cu-0.31Cr-0.29Zr-0.15Ti and Alloy 2 Cu-0.43Cr-0.39Zr (in wt.%). As there have been many literatures on Cu-Cr-Zr alloys, preparation of Alloy 2 was used as reference for mechanical property comparison and no detail on microstructure characterisation was given. The two ingots were solid solution treated at 950 °C for 60 min followed by quench in water. Ageing treatment was carried out at 450 °C for different durations (1, 2, 4, 6, 8 h).

The Microhardness was tested using a 200HVS-5 machine using a 1.961 N load for 30 s. Microstructure of three aged samples (1, 4, and 8 h) was characterised using high resolution transmission electron microscopy (HRTEM, Tecnai G2 F20, FEI). Compositions of the matrix and precipitates were measured using energy dispersive spectrometer (EDS, GENESIS, EDAX). The APT analyses were performed for needle shape samples ($0.5 \times 0.5 \times 20\ \mathrm{mm}^3$) using a local electrode atom probe (CAMECA LEAP 4000 HR). An ultrahigh vacuum ($\sim10^{-8}$ Pa), low temperature (50 K), a pulse repetition rate of 200 kHz and a pulse voltage fraction of 15% were applied. The standing voltage on the needle specimen was varied automatically in order to maintain an evaporation rate of 5 ions in every 1000 pulses. The reconstruction and quantitative analysis of APT data were performed using IVAS 3.6.12 software.

3. Results

Microhardness values of the samples at different ageing stages have been plotted in Fig. 1. It is clear that the microhardness of the two alloys increases sharply at the initial stage (0–2 h) and reaches peak values of 160 after around 2–4 h ageing. For the Cu-0.43Cr-0.39Zr alloy, the maximum microhardness is 138 HV0.2 at 4 h. When adding 0.15 wt% Ti into the alloy, the microhardness can reach 160 HV0.2 at 4 h, although less Cr and Zr are in the Cu-0.31Cr-0.29Zr-0.15Ti alloy. This indicates that Ti atoms probably have more remarkable effect on the Cr precipitates and thus enhancing the mechanical properties of Cu-Cr alloys. A sharp drop of the microhardness of the second alloy including Ti is attributed to defects in the alloy.

In order to identify the influence of Ti on the Cr precipitates, HRTEM has been used to characterise the microstructure for the Cu-0.31Cr-0.29Zr-0.15Ti alloy. Fig. 2 shows the bright field images (BEI) of the samples aged at 450 °C for 1, 4, and 8 h. In all the three samples, precipitates distribute uniformly in the domain. Also no obvious growth of the precipitates can be observed. Diffraction patterns corresponding to the three samples are presented in Fig. 2. Patterns for Cu matrix with fcc structure have been determined, while it is interesting to find that there exist no patterns for precipitates in all the three samples.

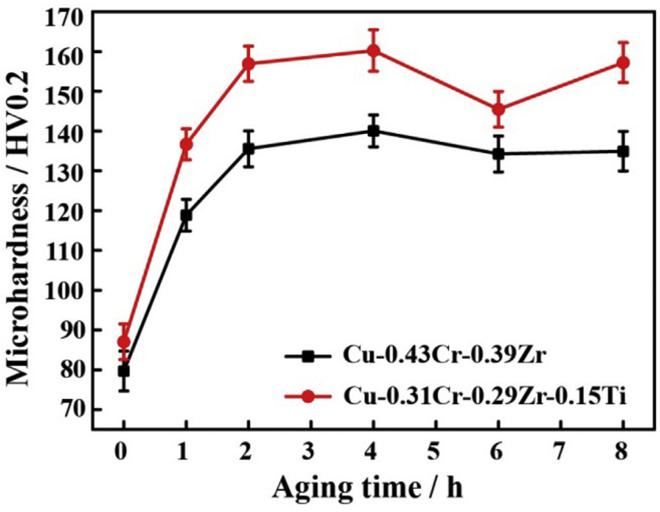

Fig. 1. Microhardness values of the samples at different ageing stages.

In order to confirm the non-growth of precipitates, bright field images with high resolution are given in Fig. 3. In the sample aged for 1 h, the precipitate is about 3–5 nm as shown in Fig. 3(a). The corresponding patterns after fast Fourier transformation (FFT) are in Fig. 3(b). Only spots standing for the fcc crystal structure have been detect. The precipitates in the samples aged for 4 and 8 h are shown in Fig. 3(d) and (g), respectively. The FFT images are further processed by blocking the high frequencies, by applying the masking on the FFT points [18] and the best filtered image obtained are shown in Fig. 3(c) and (f) and 3(i). The clear precipitates are observed. The sizes of the precipitates in both samples keep around 3–5 nm. Moreover, there is also one set of patterns representing the fcc structure can be observed in Fig. 3(e) and (h). For some additional spots appear close to the center in Fig. 3(b)、(e)、(h), which may be resulted from stack faults formed during aging.

Compositions of three areas are measured using EDS for the matrix and precipitates as listed in Table 1. Three areas are the matrix, the core of precipitates, and the matrix side of interface area (periphery of the precipitates). In spite of the accuracy and spot size of beams for the EDS, the measurement can give a rough view for the distribution of various atoms. In the matrix, 100 wt% of Cu is given without any other alloyed elements. In the matrix side of interface area (periphery of the precipitates), no Ti has been detected, but the compositions of Zr element reach 0.36, 0.70, and 0.62 wt% for the samples aged for 1, 4, 8 h, respectively. This is higher than the value of Zr composition in the alloy (0.29 wt%) which shows segregation of Zr atoms around precipitates. This is consistent with the APT observation [9,10]. In the case of the core of precipitates, high compositions of Cr can be expected. However the situation of Zr and Ti atoms are just opposite to the periphery area – few Zr atoms being detected and certain amount Ti atoms being present (0.12, 0.25, 0.14 wt%).

Nanoscaled Cr-rich precipitates are clearly shown in the 3-D reconstructed volumes in Fig. 4 using APT analyse. It is interesting to find that the sizes of precipitates are similar 2–5 nm. This is consistent with the TEM observation in Figs. 2 and 3. Also the morphologies of the Cr-rich precipitates remain ellipsoid. In Fig. 4(c), after annealing for 1 h, the tendency of segregation of Cr atoms (in purple) is obvious, and the Ti atoms (in yellow) distribute somehow evenly. But a few Zr atoms (in green) scatter here and there at the periphery of the volume. In Fig. 4(d), after annealing for 4 h, Cr atoms (in purple) and Ti atoms (in yellow) are strongly segregating into the core of the precipitates. But the Zr atoms (in green) still locate at the periphery of the precipitates. The corresponding concentration profiles of the two typical precipitates are shown in Fig. 5. For the precipitate in the sample after 1 h annealing in Fig. 5(a), the concentration of Cu decreases to 70 at.% from the interface to the precipitate core, while the Cr increases to 20 at.%. No obvious segregation of Zr or Ti atoms can be observed. For the case of 4 h annealing sample in Fig. 5(b), the concentration of Cu is only about 30 at.%, while the Cr concentration raises to 50 at.% in the core region. It should be worth noting that the concentration of Ti increases up to ~6 at.%, and Zr concentration increases slightly. The concentration of Ti is consistent with the measurement in our previous work [16]. Also the atom distribution follows the trend from the TEM-EDS results in spite of some composition deviations (see Table 1). Since the different evaporation fields make the analysis of such small precipitates difficult in APT, there could be some errors considering the composition analysis, such as very low content of Cu in the small particles. Thus several particles have been analysed to reduce aberrations. Nevertheless, the results can still make some guidance for understanding the role of those micro-alloying elements to be discussed in the following section.